Comparison between Catalytic Fast Pyrolysis and Catalytic Fast Hydropyrolysis of Arundo Donax in a Fluidized Bed Reactor

Devin Chandler

A thesis

submitted in partial fulfillment of the

requirements for the degree of

Master of Science

University of Washington

2018

Committee:

Fernando Resende, Chair

Renata Bura

Anthony Dichiara

Program Authorized to Offer Degree:

School of Environmental and Forest Sciences

University of Washington

Abstract

Comparison between Catalytic Fast Pyrolysis and Catalytic Fast Hydropyrolysis of Arundo Donax in a Fluidized Bed Reactor

Devin Chandler

Chair of the Supervisory Committee:

Fernando Resende

School of Environmental and Forest Sciences

In this work, we report the use of catalytic fast pyrolysis with HZSM-5 to convert Arundo Donax into liquid transportation fuels in an inert atmosphere, varying the temperature, the weight hourly space velocity (abbreviated WHSV, and defined as the feed rate of biomass divided by the weight of catalyst), and the pressure. We also introduced hydrogen gas as a reactant and investigated its effects on the yields at 35 bar and 400°C. Additionally, we added nickel to the HZSM-5 catalyst at loadings from 0.6 to 1.5 wt.% and investigated its effects on both catalytic fast pyrolysis and catalytic fast hydropyrolysis. Finally, we used a nickel-molybdenum HZSM-5 catalyst to determine if the molybdenum prevents the hydrocarbons from cracking to permanent gases. The goal is to understand the effects of these variables on the products of pyrolysis and increase the yield of fuel-like hydrocarbons.

The highest yield of hydrocarbons in an inert atmosphere at atmospheric pressure was obtained at 550°C (11.6 C%). As we increased the WHSV, the yields of all products remained the same until the highest WHSV tested, 3.3 hr^{-1}, at which point the yield of hydrocarbons

decreased to 6.9 C%. Increasing the pressure increased the char and gas yields. The addition of hydrogen decreased the yield of coke and increased the yield of hydrocarbons at 400°C from 4.3 to 6.2 C%. Nickel decreased the yield of liquid hydrocarbons to 1.5 C% in hydrogen gas while greatly increasing the yield of gaseous hydrocarbons, especially methane, and water, though it had little effect in inert gas. Finally, we used nickel-molybdenum HZSM-5 to increase the yield of liquid hydrocarbons in catalytic fast hydropyrolysis to 7.9 C% at 400°C.

Contents

Introduction

Need for a sustainable liquid fuel

For over a century, we have primarily fueled our transportation with petroleum-based fuels. As petroleum resources are depleted, we will need to explore alternative fuels. Such an alternative will need to be compatible with our current liquid-fuel infrastructure, cheap, and readily available. Catalytic fast hydropyrolysis (CHP) of biomass can make such a fuel. CHP breaks down lignocellulosic polymers at temperatures between 300 and 600°C into volatile organic liquids and catalytically transforms them into compatible hydrocarbon fuels in the presence of pressurized hydrogen gas and a solid catalyst, either in a single unit (*in-situ)* or in a sequence of two units (*ex-situ)*. With a sufficiently fast-growing, cheap feedstock, CHP could meet much of the transportation needs of our society.

Arundo Donax is a fast-growing herbaceous weed. It requires little input, and grows at a rate of 37.7 tons per hectare per year, which is 34.8% faster than even Miscanthus x giganteus [1]. Furthermore, there is a need to eliminate it from the habitats it is invading [2]. The fast growing rate of the feedstock could be what is necessary to economically supply fuel for our transportation sector in the near future.

Introduction to catalytic fast pyrolysis and catalytic fast hydropyrolysis

Fast pyrolysis can be represented by lumped mechanisms as shown in Figure 1. In reality, biomass undergoes thousands of reactions during fast pyrolysis, catalytic fast pyrolysis, and hydropyrolysis, but in a general sense, the process proceeds as follows: first, the lignocellulosic polymers (cellulose, hemicellulose, and lignin) breakdown in the presence of heat into oxygenated volatiles (eq 1).

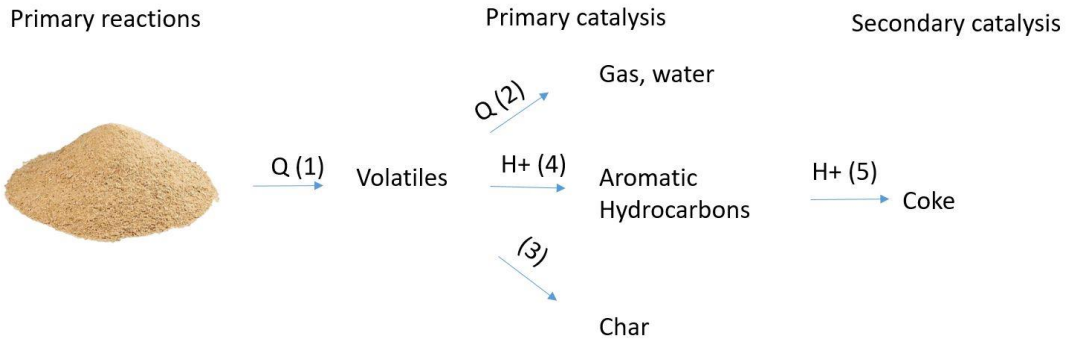

Figure 1: Lumped mechanisms of catalytic fast pyrolysis. Q indicates heat. H+ indicates an acid site on HZSM-5 catalyst. (1) is the volatilization of biomass. (2) is the cracking of volatiles to water and permanent gases. (3) is the recombination of volatiles to char. (4) is the adsorption of volatiles to the catalyst. (5) is the coke production.

Fast pyrolysis is characterized by reaction times of less than 2 seconds [3]. If the volatiles are exposed to high temperatures for too long, or if the temperature is too high, they crack into permanent gases. If the temperature is too low or the heating rate is too slow, the recombination of volatiles into char will become more favorable [3].

The addition of a zeolite catalyst, such as HZSM-5, promotes deoxygenation reactions, turning the volatiles into hydrocarbons, mainly aromatics, such as benzene, toluene, and xylene (abbreviated BTX). However, if the hydrocarbons fail to desorb, they will oligomerize into coke and remain in the pores of the catalyst, blocking the active sites [4].

Noncatalytic hydropyrolysis studies have shown that hydrogen itself has a small impact on the products of pyrolysis. Meesuk et al [5] found that more gases are produced at the expense of char. They hypothesize that the char undergoes hydrogasification in this environment. In the presence of an HZSM-5 catalyst, hydrogen does not increase liquid hydrocarbon production in semi-batch systems such as Py-GC/MS [6,7], but may limit solids production by

hydrogasification and thus could improve yields of hydrocarbons in continuous hydropyrolysis reactors [5].

Adding transition metals to HZSM-5 catalyst decreases the rate of coke production on the Brönsted acid sites, simultaneously increasing the production of saturated alkanes, especially methane [6–9].

In this work, we report the use of HZSM-5 to convert Arundo Donax into liquid hydrocarbons in an inert atmosphere, varying the temperature, the weight hourly space velocity (WHSV, the feed rate of biomass divided by the weight of catalyst), and the pressure. Then, we introduced hydrogen gas as a reactant and investigated its effects on the yields at 35 bar and 400°C. After that, we added nickel to the HZSM-5 catalyst at loadings from 0.6 to 1.5 wt.% and investigated its effects on both catalytic fast pyrolysis and catalytic fast hydropyrolysis. Finally, we added molybdenum to the Ni-HZSM-5 to investigate its ability to recombine the hydrocarbon gases. The goal is to understand the effects of these variables on the products of pyrolysis.

Literature review

To the best of our knowledge, the first use of biomass in fast pyrolysis occurred in the 1970s, when the Occidental Research Company of San Diego, CA used biomass in a pyrolysis reactor designed to convert waste products, such as plastics and rubbers, into low-sulfur fuel oil and char. Yields were poor, often only 40% liquid [10]. In the 1980s and 1990s, researchers at the University of Waterloo, led by Scott, began studying the decomposition of biomass into bio-oil, with yields as high as 80% liquid oil with a bubbling fluidized bed reactor [11]. Since then,

fast pyrolysis has been a major topic of research, showing promise for making sustainable liquid fuels.

The first instance we have found of a catalyst being used to upgrade bio-oil *in-situ* to more useful hydrocarbon products occurred in 2000, when Olazar et al used HZSM-5 to convert sawdust to liquid oil in a conical spouted bed reactor [12]. The yield of liquid hydrocarbons was 8.20 wt.%. Huber et al demonstrated the effect of temperature from 500 to 670°C and WHSV from 0.1 to 1.7 hr^{-1} of the catalytic fast pyrolysis of sawdust and found that as WSHV increased, toluene and xylene yields decreased while naphthalene yields increased. They also found a maximum of total aromatics of 14.0 C% at 600°C and 0.1 hr^{-1}. Generally, toluene yields decreased with increasing temperature while benzene and naphthalene yields increased [4].

Literature on CHP has only been available for the last few years. Much of it has been thoroughly summarized by Resende [13]. Most studies have been done via Py-GC/MS [6–8,14–16]. Gamliel et al tested the effects of catalyst properties on the products of CHP and found that acidic catalyst supports produced more aromatics and metal impregnated acidic supports made more methane and other light alkanes [14]. In another study, the same group determined that Ni-HZSM-5 solid yields decreased with increasing hydrogen pressure, gas yields increased, and liquid yields remained the same [15]. They also determined that a 3% Ni loading on HZSM-5 produced higher liquid yields when compared to a 5% loading and the unloaded support. Jan et al determined that Pd-HZSM-5 produced more C6+ hydrocarbons than HZSM-5 [7]. Most recently, Gamliel et al tested hydropyrolysis of anisole in a Py-GC/MS system with 4% Ni-ZSM-5 and found that at lower temperature and higher hydrogen pressure, the production of liquid alkanes is favored while lower hydrogen pressure favors aromatics. Higher temperature hydropyrolysis with 4% Ni-ZSM-5 produces mostly methane. Thangalazhy-Gopakumar et al

studied various transition metals impregnated on HZSM-5 at varying hydrogen pressures for hydropyrolysis at 650°C (coil temperature) [17]. With HZSM-5 without a transition metal, they found that increasing the pressure did not have any effects until they reached 27.5 bar, at which point the xylene yield decreased and the toluene increased. The total yield of hydrocarbons did not change. With Mo-ZSM-5, increasing pressure increased the yield of hydrocarbons, such as benzene, toluene, xylene and polyaromatic hydrocarbons. Comparing the different catalysts, there was not any change in total hydrocarbons yields between the Co, Mo, Ni, or Pt HZSM-5. Another study from Thangalazhy-Gopakumar et al also showed little difference in yields and composition between catalytic pyrolysis with HZSM-5 and catalytic hydropyrolysis with HZSM-5 at 550°C (coil) and 5.5 bar [6].

CHP of lignocellulosic biomass in a fluidized bed reactor has been reported by two groups so far [18–20]. Dayton et al tested NiMo on an unidentified catalyst support in a fluidized bed reactor and found a maximum of carbon efficiency of 42.0 C% at 425°C, 20 bar, and 40 vol.% H_2, which they define as the carbon yield of C4-C6 vapors plus the carbon yield of organic liquid [18]. The organic liquid at this temperature mostly consisted of polyaromatic hydrocarbons, phenolics, and monoaromatic hydrocarbons. The oxygen content was 2.5 wt.%. Marker et al tested the IH^2® system developed at the Gas Technology Institute (GTI) with a variety of feedstocks, but little information was given about the type of catalysts used and the tests varied multiple conditions at a time, making comparisons difficult [19]. Further testing showed that scaling from a bench scale reactor to a 50 kg/day pilot reactor did not reduce the yield or quality of gasoline and jet-fuel range hydrocarbons. The pilot scale reactor was tested for 800 hours without change to the yields [21].

GTI performed a techno-economic analysis (TEA) of the IH^2 process and determined that liquid transportation fuels could feasibly be made at a cost of $1.64/gallon in 2007 USD [20].

Non-catalytic hydropyrolysis has also been studied by various groups, notably Meesuk et al, who found that hydrogen at atmospheric pressure in the absence of catalyst slightly reduces the bio-oil and char yield and increases the gas yield [5].

Experimental Methods

We prepared the biomass by grinding the stalks of Arundo Donax into particles less than 1 mm, averaging 0.34 mm in diameter, with a hammer mill (Thomas Wiley, Philadelphia, PA). We measured the ash content to be 3.91 wt.% dry basis, by performing the NREL method outlined in TP-510-42622 [22]. We measured the moisture content by weight difference before and after drying at 105°C overnight in an oven (Blue M, Blue Island, IL) and found it to be 5.81 wt.% on a dry basis.

The HZSM-5 pellets were commercially available (Pingxiang Naike, Pingxiang, CN) with a Si/Al ratio of 38. The diameter of the pellets was 2-3 mm. We prepared the Ni-HZSM-5 by wet impregnation of the pellets. We did this by mixing nickel nitrate hexahydrate (Sigma Aldrich, St. Louis, MO) with deionized water. For all catalysts, we used 1.25 mL of water per gram of catalyst. To prepare catalysts with nickel loadings of 1.5 wt.%, 1.0 wt.% and 0.6 wt.% Ni-HZSM-5, we used 0.75 g, 0.30 g, and 0.15 g of nickel nitrate hexahydrate per gram of catalyst, respectively. We slowly dripped the solution onto the HZSM-5 pellets while stirring the pellets. This process took one hour to complete. Upon completion, we thoroughly rinsed the pellets with deionized water, dried them overnight at 105 °C, and calcined them in air at 550 °C for 5 hours in a muffle furnace (Thermo Fisher Scientific, Waltham, MA). To produce the NiMo-

HZSM-5, we used 0.3 g ammonium molybdate tetrahydrate per gram of catalyst and slowly dripped the solution onto previously prepared 1.4 wt.% Ni-HZSM-5 using the same procedure as for the nickel catalyst. The result was a 2.7 wt.% Mo, 1.4 wt.% Ni HZSM-5. We reduced the nickel and/or molybdenum sites of the catalyst in hydrogen in the fluidized bed during the heat-up time (4 hrs.).

We performed ICP-AES using the EPA 200.7 [23] method to determine the nickel and molybdenum content of the catalyst after calcining. We performed BET analysis of the catalyst to determine the surface area and pore dimensions.

We performed catalytic fast pyrolysis (CFP) in a fluidized bed reactor system as shown in Figure 2. A magnetic stirrer in the hopper aided the biomass onto the auger. The auger carried biomass from the hopper to a funnel where it was pneumatically forced in the reactor. The reactor bed contained 200 g of 2-3 mm spherical catalyst mixed with 200 g of 100-500 µm alumina sand (Kramer Industries, Piscataway, NJ) to assist in fluidization. We preheated the gas going into the reactor with a heating tape (HTS Amptek, Stafford, TX). An electric furnace (Carbolite Gero, Sheffield, UK) surrounded the reactor to provide heat to the reaction. The products were carried from the reactor to the cyclone via a transfer line, which separated the char. We maintained the transfer line and cyclone temperatures at 275-350°C throughout the run with additional heat tapes. The non-solids were then carried to the condensation system consisting of an impinger, three double-pipe condensers (the last two filled with 6 mm glass beads (Fisher Scientific, Hampton, NH)), and three methanol-filled bubblers. A chiller (Thermo Fisher Scientific, Waltham, MA) provided water at 5°C to the double-pipe condensers. The vapor at the first condenser was usually at 10-20 °C in the atmospheric pressure experiments and 100-150°C in the higher-pressure experiments. The second and third condensers were both

below 10°C for the atmospheric pressure experiments. At higher pressures, the second condenser was usually 20-40°C and the third was around 10°C. We placed the methanol bubblers in a dry-ice bath to ensure maximum dissolution of products into the methanol. Finally, the permanent gases went through a coalescing filter (Swagelok, Solon, OH) and vented from the system. We collected a portion of the vented gases in gas sampling bags (Restek, Bellefonte, PA) throughout the entire run.

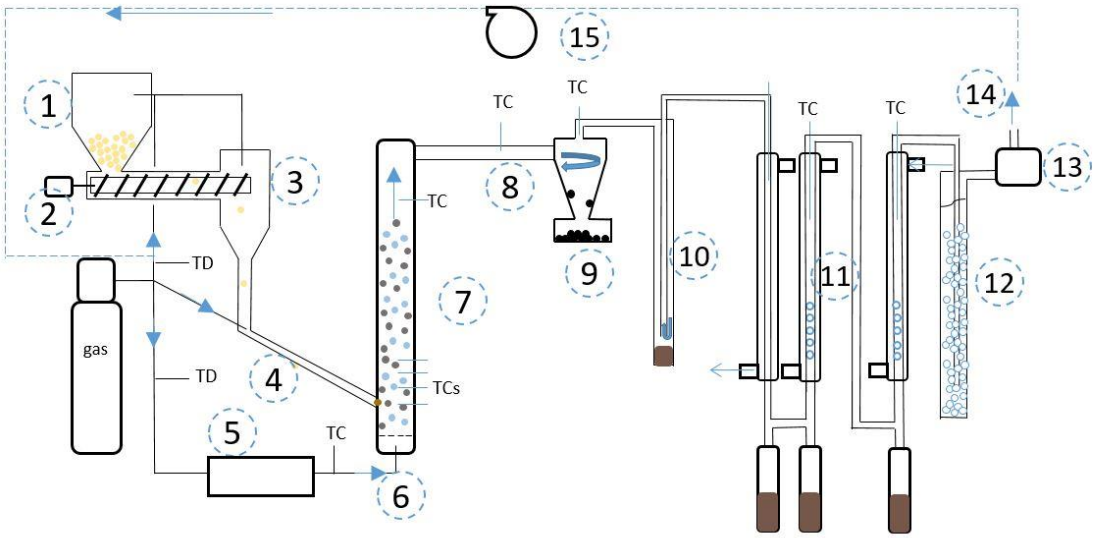

Figure 2: Reactor schematic. 1) Biomass hopper. 2) Auger motor. 3) Feed funnel. 4) Feed line. 5) Pre-heater (high pressure only). 6) Fluidizing gas. 7) Fluidized bed reactor with catalyst and sand. 8) Transfer line. 9) Cyclone separator. 10) Impinger (cooled by water bath in high-pressure experiments). 11) Double-pipe condensers. 12) Methanol bubblers (atmospheric pressure) or glass-bead-filled impingers (high pressure). 13) Coalescing filter. 14) Exhaust (atmospheric pressure) 15) gas booster (high pressure). TC: thermocouple. TD: transducer

After the run was completed, we collected the gas bags and analyzed their contents with a GC-TCD/FID 2014 (Shimadzu, Kyoto, JP) using a Supelco 60/80 Carboxen 1000 packed column (Supelco Analytical, Bellefonte, PA). We calibrated for carbon monoxide, carbon dioxide, ethylene, and nitrogen. We collected and weighed liquids in the collectors. We shook their contents thoroughly and dissolved a sample into methanol for GC-MS/FID 2010

(Shimadzu, Kyoto, JP) analysis using a capillary column as described elsewhere [24]. We individually calibrated 48 compounds and assumed some compounds to have the same response factors as those with a similar chemical structure (i.e., indene and indane, dimethylfuran and vinylfuran, etc.). Furthermore, we analyzed samples of the collected liquids in a Mettler Toledo V20 Karl Fisher Titrator (Mettler Toledo, Columbus, OH) for the yield of water. We accounted for liquids that adhered to the interior walls of the tubing of the condenser system by weighing all components before and after the reaction. We then dissolved the adhered liquids in methanol and analyzed them by GC-MS/FID. We ran the contents of the bubblers through the GC-MS/FID without further dilution. We collected the char from the cyclone separator, transfer line, and reactor. We separated the coked catalyst from the rest of the bed by sieving in order to differentiate coke and char since the coked catalyst has a much larger diameter (2-3 mm) than the sand and char particles. We burned samples of the char from each collection point at 600°C for 6 hours in air to determine the amount of organic char and the amount of ash or sand. We analyzed samples of each component in a CHN 2400 elemental analyzer (Perkin-Elmer, Waltham, MA) to determine the elemental content of the char. Samples of coked catalyst underwent the same procedures to determine the coke yield and elemental composition.

We performed some changes to the reactor system and analysis to make it suitable for high-pressure experiments. For ease of fluidization, we decreased the reactor inner diameter from 3.8 cm to 2.5 cm, and switched from inert nitrogen to inert helium. Rather than venting the gas at the end of the system, we used a Maximator gas booster (Maxpro Technologies, Fairview, PA) to recycle the gas back to the reactor. This may have affected the gas composition, as the gaseous products went through the reactor multiple times. Finally, to prevent the methanol bubblers from releasing methanol vapor through the reactor system, we replaced the methanol with 3 mm glass

beads. We took gas samples at the end of the run instead of throughout the run. We also placed the furnace before the reactor to increase heat transfer to the gas feed since pre-heating the gas with heating tapes was insufficient at high pressure. High temperature heating tapes (HTS Amptek, Stafford, TX) wrapped around the reactor then maintained the reaction temperature through the experiment. For high-pressure experiments, we analyzed the gas samples in a GC/TCD-FID with a HP Plot capillary column (Agilent Technologies, Santa Clara, CA) to account for C3+ vapors, whereas in the low-pressure CFP experiments, we assumed these to be negligible.

We performed the CFP experiment at 550°C, atmospheric pressure, with HZSM-5, and a WHSV of 1.1 in triplicates to determine the standard deviations. WHSV is defined in Equation 1. We assumed the standard deviations to be independent of the variables tested. We determined statistical significance in the data by two sample t-tests for all reported yields. We performed all analytical testing of products at least two times. Any differences in data that are determined to be insignificant are treated as equal. All data are reported on a carbon yield basis except where noted.

$$WHSV\ (hr^{-1}) = \frac{feed\ rate\ of\ biomass\ in\ kg/hr}{mass\ of\ catalyst\ in\ kg}$$

Equation 1: Definition of weight hour space velocity

Results and Discussion

The characterization of the Arundo Donax used can be found elsewhere [25]. The same source also presents the results of non-catalytic fast pyrolysis at various temperatures. The main liquid products of non-catalytic fast pyrolysis are oxygenated compounds, mainly acetic acid. In this case, the organic liquid yields are highest at the lowest tested temperature, 400°C (40.5 wt. %). This temperature of highest yields is lower than for more biomass feedstocks, mainly

because of the high content of potassium (1.06 wt.%) [25]. No liquid hydrocarbons were produced in non-catalytic fast pyrolysis of Arundo Donax.

Catalytic fast pyrolysis (CFP)

Effect of Temperature

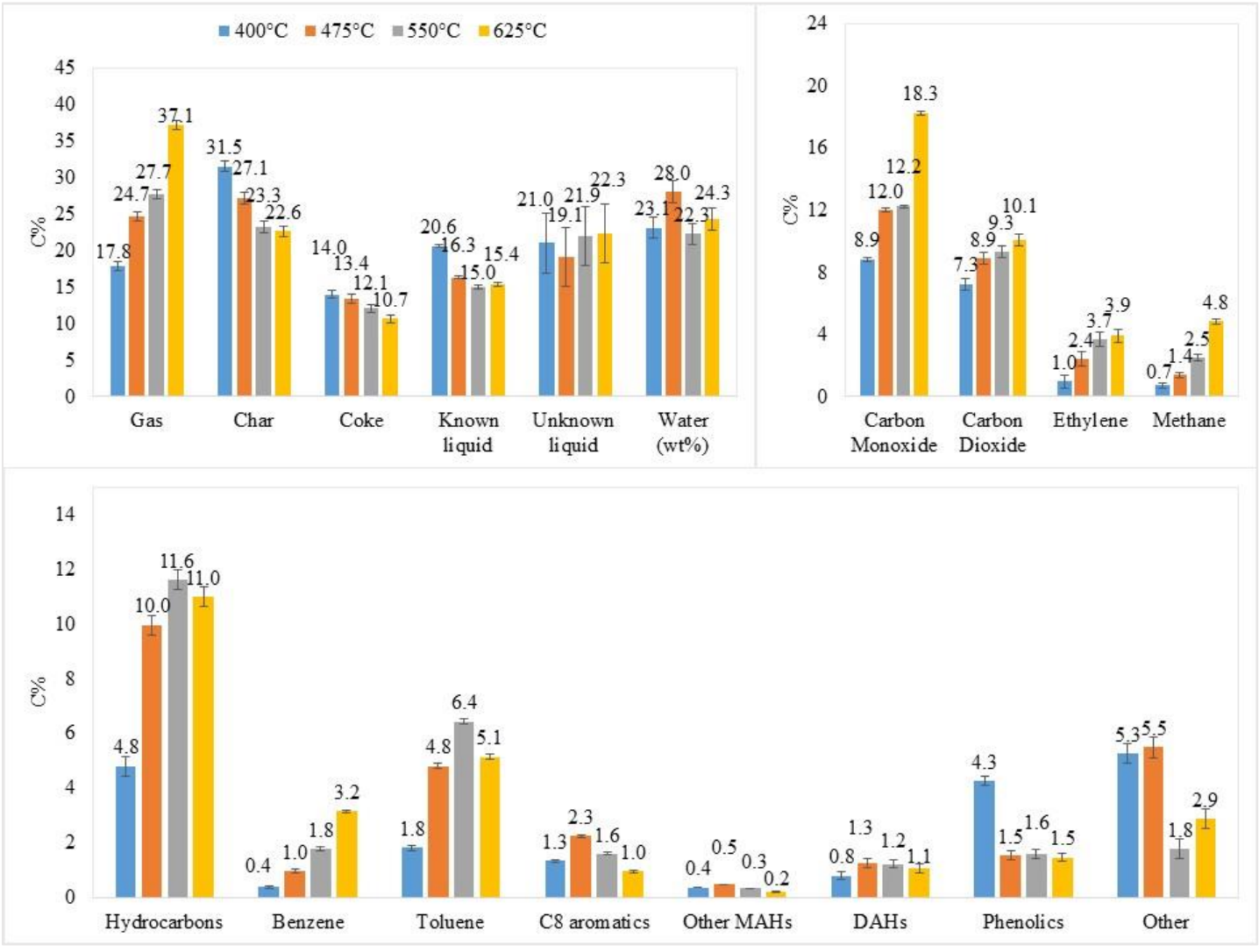

Figure 3: Yields of CFP with varying temperature. Top left: total yields. Top right: Gas yields. Bottom: major liquid compounds. MAH: mono-aromatic hydrocarbon. DAH: di-aromatic hydrocarbon. The carbon balances are between 98.6-108.1 C%.

We performed catalytic fast pyrolysis of *A. donax* in nitrogen gas at atmospheric pressure and evaluated the effect of temperature, weight hourly space velocity (WHSV), pressure, and catalyst. We used 550°C, 1.0-1.2 hr^{-1} WHSV, 1 bar, and HZSM-5 catalyst as the base case experiment, which we performed in triplicate.

The yields of products from CFP at varying temperatures are shown in Figure 3. For the base case, the carbon balance was 99.9 C% ± 3.4 and the mass balance was 98.0 wt.% ± 5.5. The carbon yields are as follows: 23.3 C% ± 0.1 char, 12.1 C% ± 0.6 coke, 15.0 C% ± 0.2 known liquid, 21.9 C% ± 4.0 unknown liquid (totaling 36.9 C% ± 4.0 liquid), and 27.7 C% ± 0.6 gas. Known liquids were determined by GC/MS-FID analysis and total liquid carbon was quantified by CHN analysis. We quantified unknown liquid carbon by subtraction. We believe the unknown liquid to be oligomeric tars composed of molecules that are too large to be analyzed via GC/MS-FID. The water yield was 22.3 wt.%. The 15.0 C% known liquids are composed of 11.6 C% ± 0.4 hydrocarbons, 1.6 C% ± 0.2 phenolics, and 1.8 C% ± 0.4 other oxygenates such as acetic acid, levoglucosan, and furan. The hydrocarbons produced were 6.4 C% ± 0.1 toluene, 1.8 C% ± 0.1 benzene, 1.6 C% ± 0.0 C8 aromatics (xylenes, ethylbenzene, styrene), 0.3 C% ± 0.1 other monoaromatic hydrocarbons (MAHs, C9 and C10 aromatics), and 1.2 C% ± 0.2 diaromatic hydrocarbons (DAHs). The gases produced were 12.2 C% ± 0.1 carbon monoxide, 9.3 C% ± 0.4 carbon dioxide, 3.7 C% ± 0.4 ethylene, and 2.5 C% ± 0.2 methane.

As the temperature increased, so did the total yield of gases and the yields of each component of the gas. Carbon monoxide is the most prevalent gas, followed by carbon dioxide. These make up 8.9 C% and 7.3 C% of the yields at 400°C and 18.3 C% and 10.1 C% of the yields at 625°C. The most dramatic increase occurs in the yield of methane, which increases from 0.7 C% to 4.8 C% when the temperature increases from 400°C to 625°C. This indicates that

increasing the temperature increases the prevalence of cracking reactions. The char and coke yields decrease with increasing temperature, from 31.5 C% and 14.0 C% at 400°C, to 22.6 C% and 10.7 C% at 625°C, respectively, due to a reduction in the extent of recombination reactions. The yield of known liquids decreases with increasing temperature until it plateaus at 550°C. This aligns with our previous research showing that *A.* donax produces the most volatiles from non-catalytic fast pyrolysis at 400°C [25]. However, because increasing the temperature also increases the activity of the catalyst, the hydrocarbon yield increases with increasing temperature until it plateaus at 550°C at a yield of 11.6 C%, when the increase in catalytic activity producing liquid hydrocarbons begins to be undermined by the increase in the extent of cracking reactions converting the volatiles into permanent gases. Benzene and di-aromatic hydrocarbon (DAH) yields increase with increasing temperature to a maximum of 3.2 C% and 1.1 C% at 625°C. Toluene reaches a maximum at 550°C with a yield of 6.4 C% and C8 aromatics at 475°C with a yield of 2.3 C%. At high temperatures, it is likely that the methyl groups on toluene and C8s are cracked to form methane and benzene. The high temperature also cracks polyaromatic coke and char to form more diaromatic hydrocarbons. The lowest temperature tested, 400°C, yielded less aromatic hydrocarbons and more phenolics and other oxygenated liquid products, indicating low catalytic deoxygenation. Oxygenated liquids are generally present in lower yields at higher temperature.

Furthermore, non-catalytic fast pyrolysis of *A. donax* produced very little ethylene at all, and the yield of carbon monoxide was about half that of carbon dioxide, whereas with a catalyst, ethylene is produced in significant quantities and carbon monoxide is more prevalent than carbon dioxide [25]. Therefore, we can conclude that ethylene and carbon monoxide are products of the

catalytic reactions. The carbon monoxide is likely a result of the catalytic decarbonylation at the acid site while the ethylene is likely a product of the cracking of unsaturated hydrocarbons.

Carlson et al tested the effects of temperature as well on CFP of pine sawdust and found a maximum of liquid hydrocarbons at 600°C of 11.0 C% (at a WHSV of 0.2 hr^{-1}) [4]. This aligns well with our findings, which is interesting given the presence of alkali metals in *A. Donax*, which we have previously shown to reduce organic liquid yields by promoting secondary reactions [25]. It appears that the inorganics affect mostly non-catalytic fast pyrolysis, indicating that perhaps the alkali metals only act on the less stable oxygenated volatiles.

Effect of WHSV

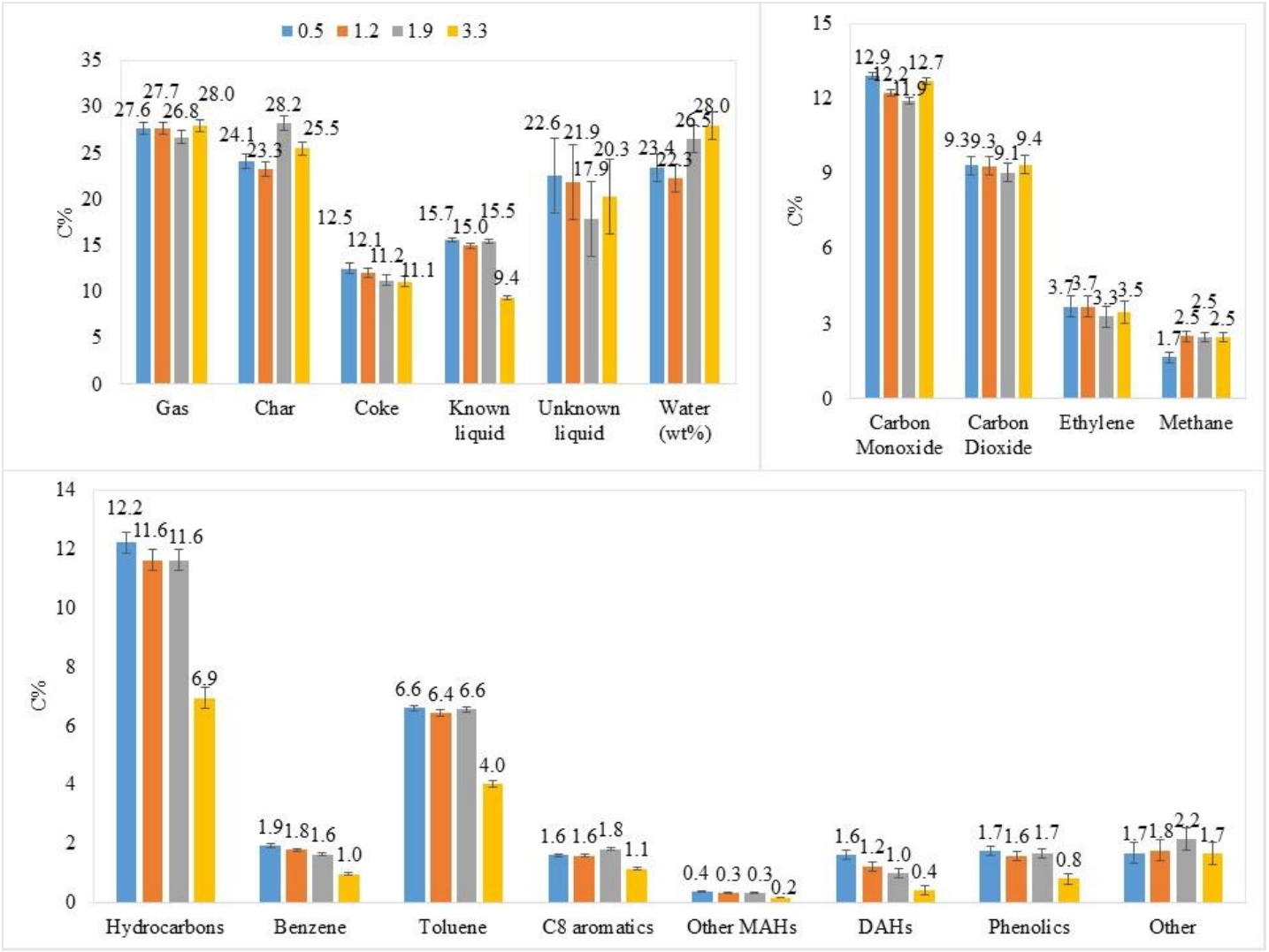

Figure 4: Results of CFP at varying weight hourly space velocities (in hr^{-1}). Top left: total yields. Top right: gas yields. Bottom: major liquid compound yields. The carbon balance is 94.3-102.4 C%.

The yields of products from CFP at varying WHSV are given in Figure 4. Decreasing the WHSV from 1.2 to 0.5 hr^{-1} by adjusting the flow of biomass into the reactor yielded slightly more carbon monoxide (12.9 C%) and less methane (1.7 C%) than the base case (12.2 and 2.5 C%, respectively). It also increased the yield of DAHs (1.6 C% at 0.5 hr^{-1} and 1.2 C% at 1.2 hr^{-1}). When we increased the WHSV to 1.9 hr^{-1} from the base case, production of char and C8s increased from 23.3 C% to 28.3 C% and from 1.6 C% to 1.8 C%, respectively. Yields of carbon

monoxide and benzene decreased to 11.9 C% and 1.6 C%, respectively. All other yields remained the same.

A further increase to 3.3 hr^{-1} seemed to have overwhelmed the acid sites of the catalyst at this point, with yields of aromatic hydrocarbons drastically decreasing from 11.6-12.2 C% at the lower WHSVs to 6.9 C% at 3.3 hr^{-1}. It appears that there are sufficient acid sites for conversion of the biomass until the WHSV exceeds 1.9 hr^{-1}. Above this WHSV, the concentration of volatile oxygenates is too high for the available acid sites, preventing a significant portion of the volatiles from being converted into aromatic hydrocarbons.

Carlson et al found that as WHSV increases in CFP of pine sawdust, MAH yields decrease or stay the same from 0.1 to 1.7 hr^{-1}, and DAH yields increase [4]. The increase in DAHs does not align with our results. The yields of DAHs from *A. donax* CFP are lower than Carlson reports for pine at nearly all conditions. This may be because the salts present in *A. donax* inhibit the formation of DAHs on the catalyst. With increasing WHSV, this affect is possibly increased due to a higher rate of salts entering the reactor bed. In the present work, all yields of hydrocarbons decrease together at WHSV above 1.9 hr^{-1} but remain nearly the same below that.

Effect of Pressure

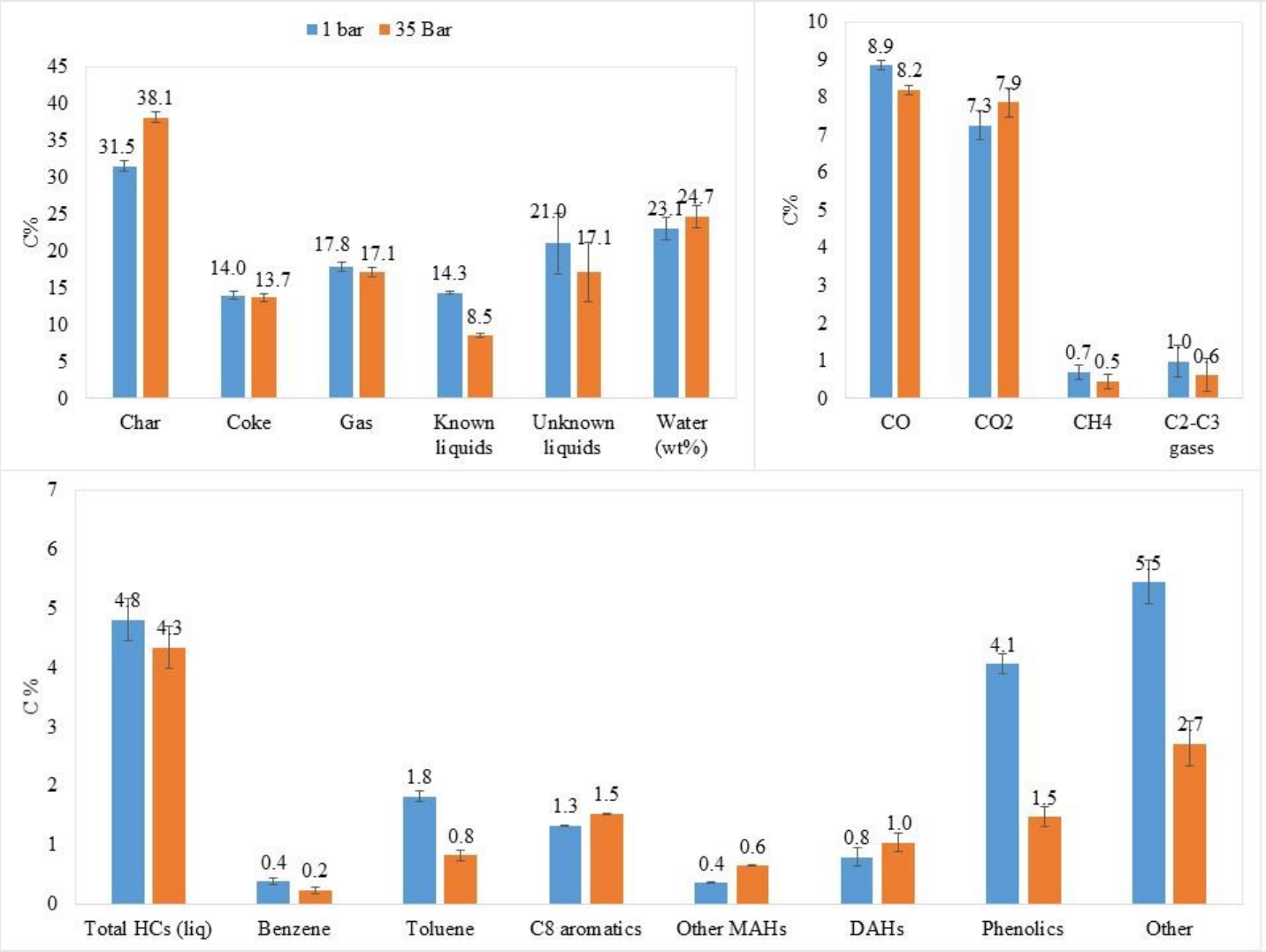

Figure 5: Results of CFP at atmospheric pressure and 35 bar. Top left: total yields. Top right: gas yields. Bottom: Major liquid compounds. The carbon balance was 98.6 C% and 94.5 C%, respectively

We performed high pressure CFP (in He gas) of Arundo Donax at 400°C and 35 bar and the results are shown in Figure 5 along with the results from atmospheric pressure CFP (in N_2 gas) at 400°C for comparison. Char yields increase from 31.5 C% to 38.1 C% at the higher pressure. Known liquid yields decreased from 14.3 C% to 8.3 C%, especially the phenolics and oxygenates, which decreased from 4.1 and 5.5 C% to 1.5 and 2.7 C%, respectively. It seems that at higher pressure, the extent of recombination reactions is higher, especially recombination of oxygenated liquids. C8 aromatic yields, other MAHs (C9+) and DAHs increased slightly while

toluene yields decreased from 1.8 C% to 0.8 C% and benzene yields decreased slightly. The higher pressure appears to contribute to recombination and alkylation of the aromatics, favoring larger branched aromatic structures over the smaller C6 and C7 aromatics. Gamliel et al reported an increase in solid yields and decrease in gas yields while liquid yields remained the same when increasing the pressure of CFP from 0 to 31 bar [15]. In the Py-GC/MS system they used, the higher pressure likely affected the heat transfer through the quartz tube, reducing cracking reactions of the volatiles while promoting recombination instead.

Results of catalytic fast hydropyrolysis (CHP)

Effect of Hydrogen

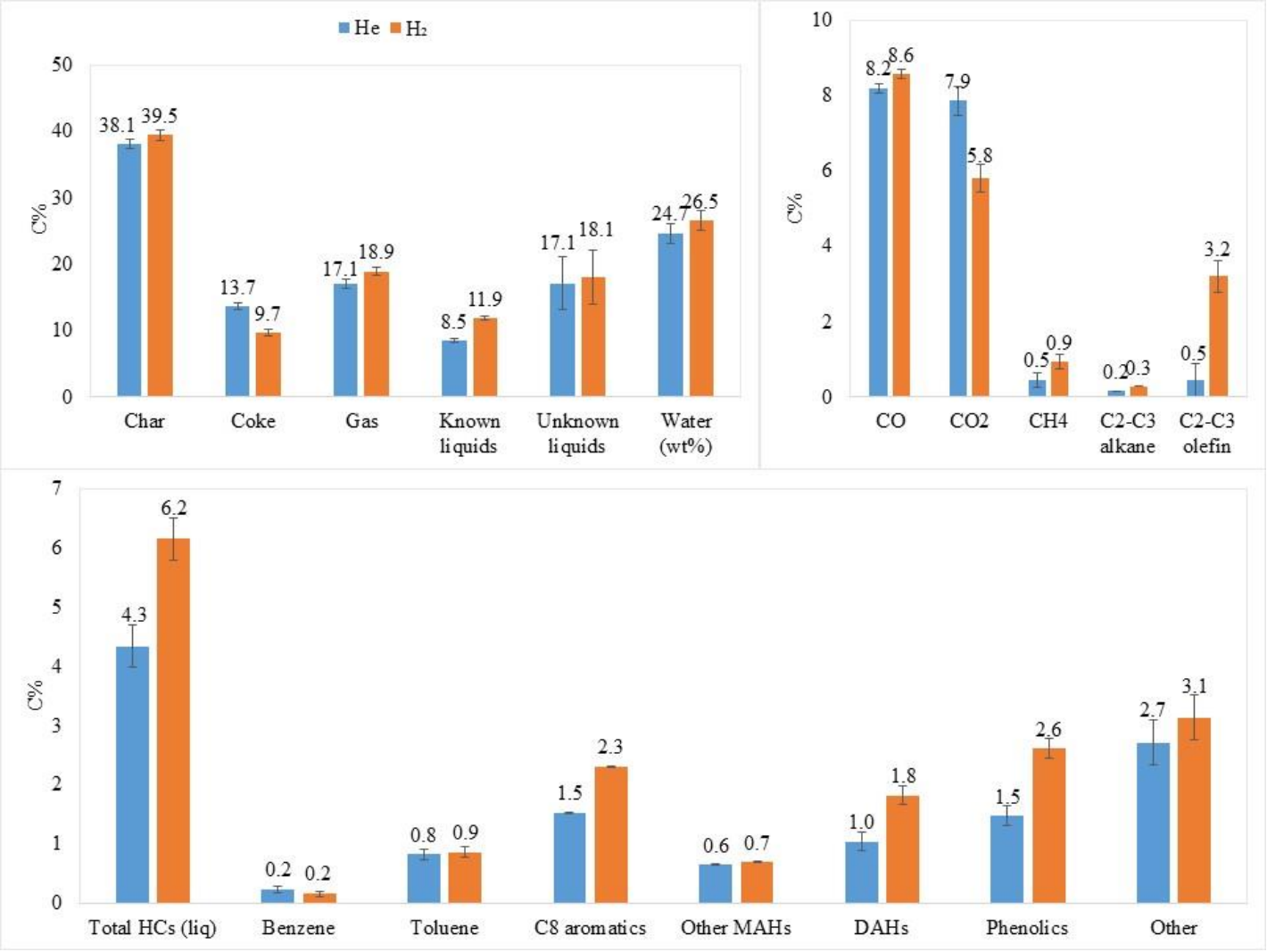

Figure 6: Comparison of results from high pressure CFP and CHP at the same conditions. Top left: total yields. Top right: yields of gaseous products. Bottom: yields of liquid products. Standard deviations for alkanes are not given because they were not produced in the base case. The carbon balances for these experiments are 94.5 and 98.0 C% for helium and hydrogen, respectively.

Comparing CFP at high pressure and a similar CHP experiment, which were performed at 400°C, 35 bar, 1.1 $^{hr-1}$, and in the presence of HZSM-5 reveals that the hydrogen gas leads to an increase in the production of hydrocarbons, from 4.3 C% to 6.0 C% over helium, especially for C8 aromatics and DAHs, which nearly doubled in yield. The yields of C2-C3 olefin gases increased from 0.5 to 3.2 C% in CHP relative to CFP while the yield of carbon dioxide decreased

from 7.9 to 5.8 C%. The coke yield decreased from 13.7 C% to 9.7 C% and the yield of phenolics increased from 1.4 C% to 2.4 C%. The hydrogen gas seems to be reducing the coking reactions and allowing for higher catalytic activity, increasing the yield of aromatic hydrocarbons, phenolics (which could be an intermediate catalytic deoxygenation product), and olefinic gases. Furthermore, the deoxygenation of the pyrolysis vapors is not producing as much carbon dioxide and is instead producing more water and phenolics. This leaves more carbon available to be converted to hydrocarbons.

The decreased rate of coking could be a result of the presence of hydrogen radicals, which cap reactive volatiles, reducing the extent of condensation reactions. Because of this, the catalyst is not deactivated as quickly during the experiment and therefore it yields more zeolite adsorption products such as BTX and ethylene. However, hydrogenation appears to be mostly limited to carbon-oxygen bonds, as the aromatic and olefin hydrocarbons do not saturate to become alkanes. It is possible that the concentration of hydrogen radicals is too small to disrupt the double bonds between carbon atoms. Furthermore, as Jan et al show [7], hydrogenation is typically favored at temperatures below 400°C. Using this information, we can add another branch to our reaction schematic in Figure 1, indicating that hydrogen radicals form olefinic gas and water from adsorbed volatiles. These reactions compete with the formation of coke.

Effect of Ni on HZSM-5 CFP

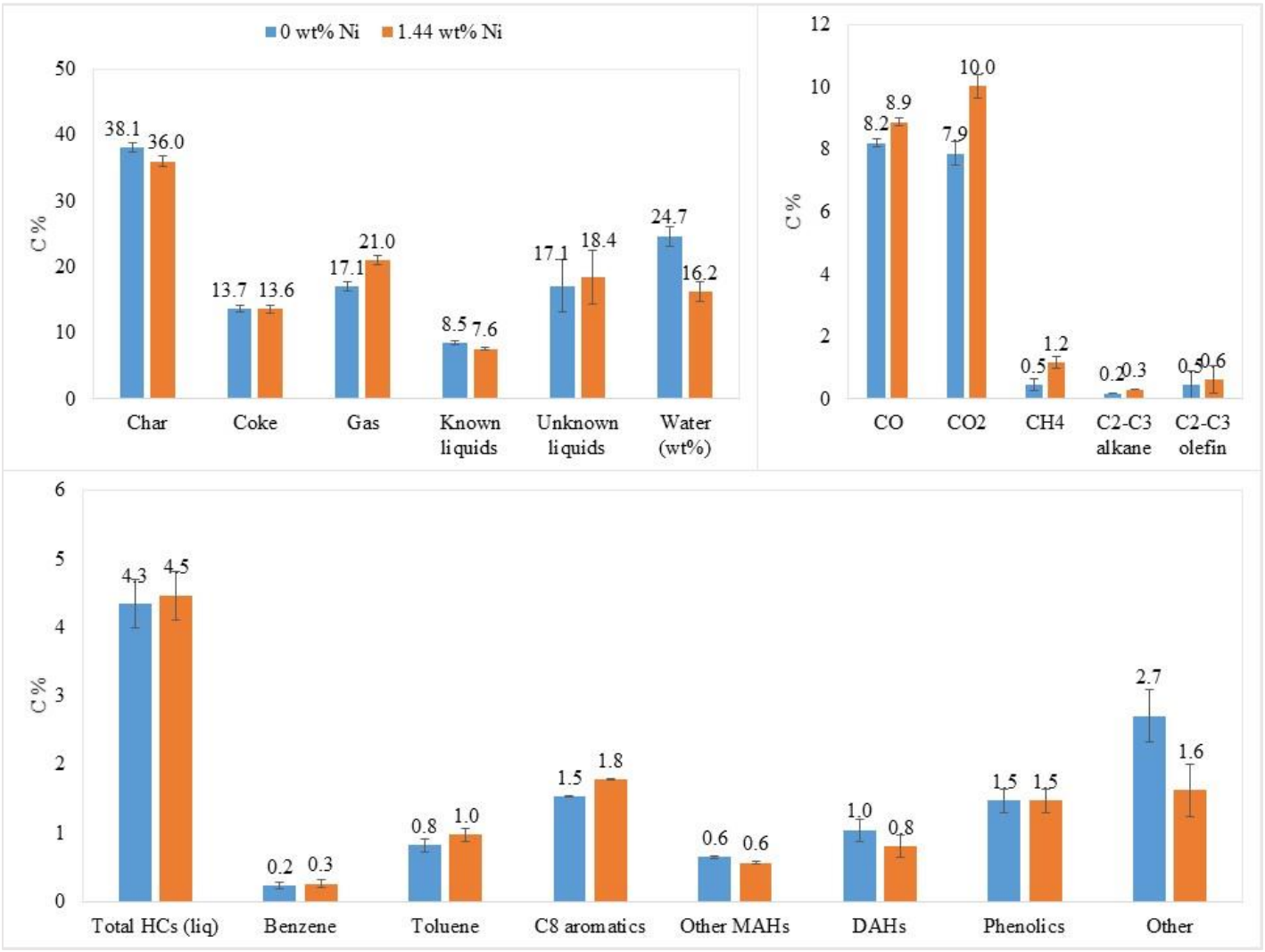

Figure 7: Yields from CFP with HZSM-5 and 1.44 wt% Ni-HZSM-5. Top left: total yields. Top right: gas yields. Bottom: major liquid compounds. Carbon balances are 94.5 and 96.6 C%, respectively.

The yields from catalytic fast pyrolysis with Ni-ZSM-5 are shown in Figure 7, with the yields from CFP with HZSM-5 for comparison. Each experiment was performed at 400°C, 35 bar, and 1.1 hr^{-1}. There was little effect on most yields from the addition of nickel to the catalyst in inert gas. All the gas yields increased except for the olefinic gases, which remained the same. The carbon dioxide yield increased the most notably, from 7.9 to 10.0 C%. The char yield decreased slightly, from 38.1 to 36.0 C%, as did the other oxygenated liquids, from 2.7 to 1.6

C%. Water yields decreased from 24.7 to 16.2 wt.%. It appears that the nickel can aid slightly in cracking char and oxygenated liquids. In the absence of hydrogen, it also seems to promote decarboxylation and decarbonylation reactions to the detriment of water yields.

Effect of Ni on HZSM-5 CHP

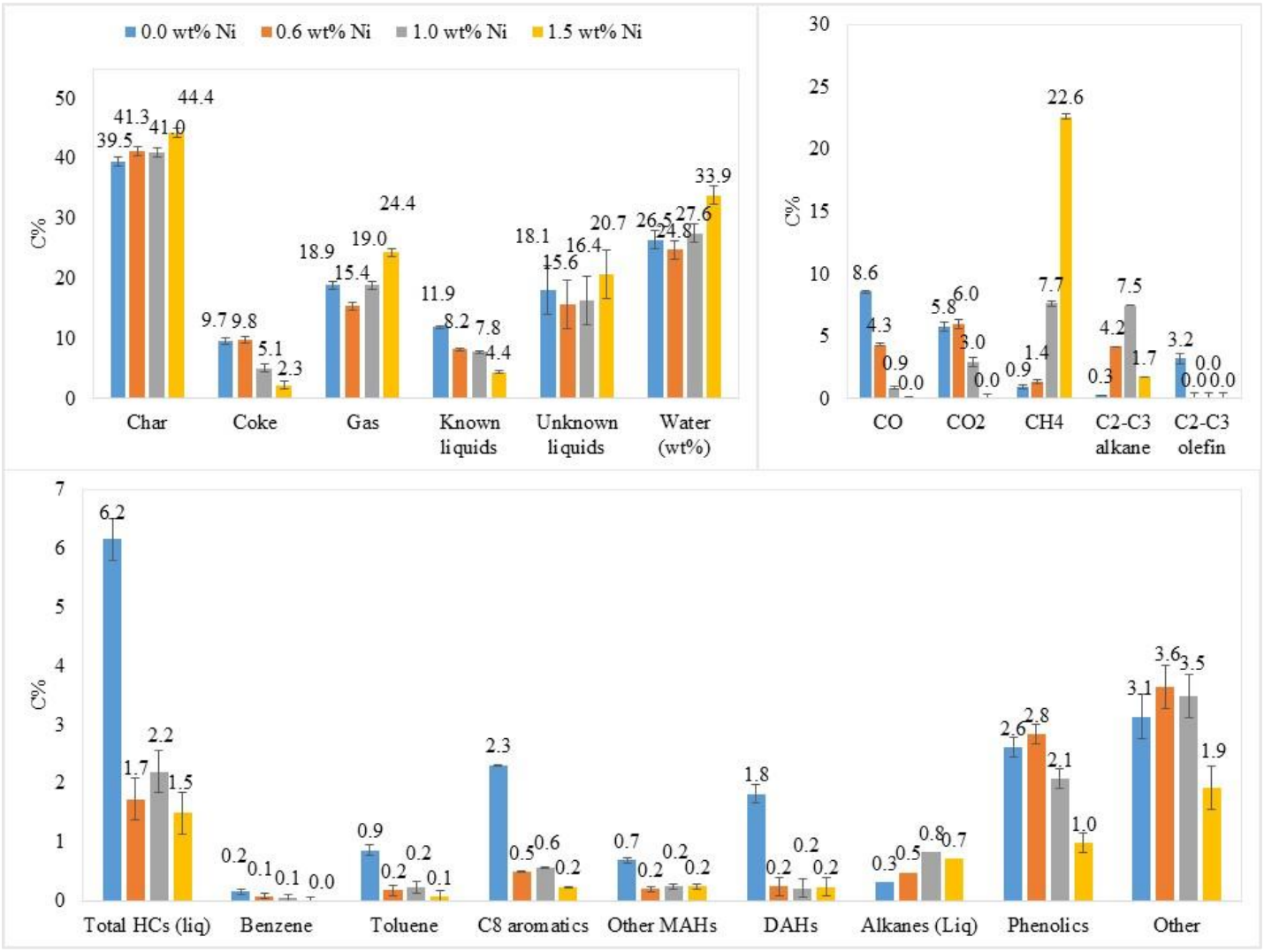

Figure 8: Effect of nickel loading of HZSM-5 on CHP yields. Top right: total yields. Top left: gaseous yields. Bottom: major liquid compounds. The carbon balances of these experiments are all between 89.2 C% and 98.0 C%.

Figure 8 gives the yields of CHP with varying nickel loadings of the HZSM-5 catalyst. As the nickel loading on the catalyst increases from 0.0 to 0.6 wt.%, the char yield slightly increases from 39.5 to 41.3 C%, remaining the same when the nickel increases to 1.0 wt.%, then

increasing again to 44.4 C% when the nickel loading increases to 1.5 wt.%. The coke yield remains at 9.8 C% when the nickel loading is increased to 0.6 wt.%, but then decreases to 5.1 C% when the nickel loading is increased further to 1.0 wt.%, then to 2.3 C% at 1.5 wt.% Ni. Nickel appears to be slightly promoting char formation while inhibiting coking.

The gas yield decreases from 18.9 to 15.4 C% with an increase in nickel from 0.0 to 0.6 wt.%, then increases to 24.4 C% when the nickel content increases to 1.5 wt.%. Specifically, the carbon monoxide decreased from 8.6 C% with 0.0 wt.% nickel to 0.0 C% at the highest loading, indicating a decrease in deoxygenation by decarbonylation. However, the carbon dioxide yield remained at 6.0 C% when nickel is introduced at a loading of 0.6 wt% before decreasing with increasing nickel loading to 0.0 C% at 1.5 wt.% Ni. The olefinic gases disappeared entirely from a yield of 3.2 C% just from the addition of 0.6 wt% Ni. The alkane gases increased from 0.9 to 22.6 C% at the maximum nickel loading for methane. When the nickel content increased to 1.0 wt.%, the yields of ethane and propane combined increased from 0.3 to 7.5 C%, but then decreased to 1.7 C% when the nickel content increased to 1.5 wt.%.The changing trends in the gas yields indicates competing reactions caused by the presence of nickel. At the lowest loading, the nickel is promoting hydrogenation of the olefinic gases and inhibiting decarbonylation, however it has not effect on decarboxylation. It is producing more alkane gases then can be explained by olefinic hydrogenation, which indicates cracking of other products. When the nickel loading is increased further, the decarboxylation begins. Meanwhile, the cracking reactions increase dramatically, affecting even the ethane and butane yields.

The known liquids decrease from 11.8 to 4.4 C% when the nickel loading increases from 0.0 to 1.5 wt%. This is likely the result of cracking, which helps to explain the increase in alkane gas yields. The liquid hydrocarbon yields decrease from 6.2 to 1.5 C%. All categories of

aromatic hydrocarbons decrease to nearly zero, while the alkane liquids increase slightly from 0.3 to 0.7 C%. The aromatic hydrocarbons seem to be saturating and cracking to permanent gas hydrocarbons. Given that nickel is shown to not greatly affect the yields of CFP, we conclude that the nickel sites mostly act on the diatomic hydrogen gas, weakening the bonds and producing more hydrogen radicals. These hydrogen radicals then attack the organic bonds, starting with the double carbon bonds, then attacking the aromatic bonds. At the highest nickel loadings, even the oxygenated liquids are cracked to water and hydrocarbon gases, indicating that the concentration of hydrogen radicals is sufficient to affect even the volatiles that do not adsorb on the acid sites of the catalyst. Finally, the water yield increases from 26.5 to 33.9 wt.% with the increasing nickel loading. At this high nickel loading, the hydrogen radicals are able to overcome the previously shown effects of the nickel sites on water production allowing it to be more prevalent than without hydrogen present.

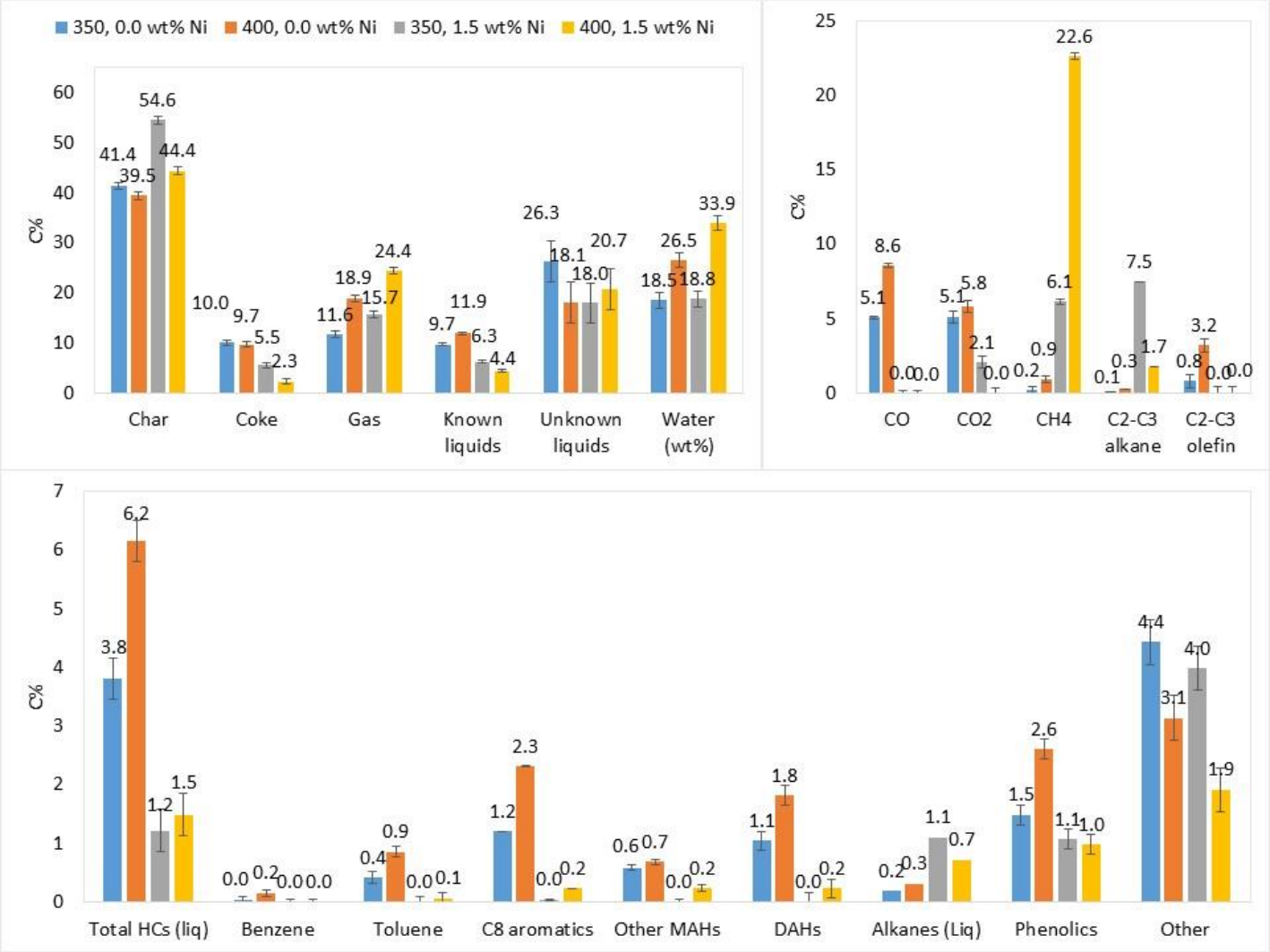

Figure 9: Effects of temperature (in °C) on yields of CHP with HZSM-5 at two different nickel loadings. Top left: total yields. Top right: gaseous yields. Bottom: major liquid compounds. The carbon balances were all between 96.1 and 100.0.

When the temperature of pure hydrogen gas without a catalyst increases from 350°C to 400°C, Colorado State University's equilibrium calculator [26] estimates that the molar concentration of hydrogen radicals increases from 4.02×10^{-17} to 9.44×10^{-16} – a 24-fold increase. The result of this increase can be highlighted by comparing the yields of CHP with HZSM-5 at 350°C and 400°C in Figure 9. The gas yield increases from 11.6 C% to 18.9 C%. Most notably, we see increases in carbon monoxide (5.1 C% to 8.6 C%), methane (0.2 C% to 0.9 C%), and olefins (0.8 C% to 3.2 C%), which are the gaseous products of catalytic

deoxygenation. We also see an increase in total hydrocarbons from 3.8 C% and 6.2 C%, driven by increases in all aromatic hydrocarbons. Furthermore, catalytic activity is increased, as shown by the decrease in other oxygenates from 4.4 C% to 3.1 C%. This demonstrates the ability of hydrogen radicals to perform hydrodeoxygenation, producing more hydrocarbons and less oxygenates, especially at higher radical concentrations.

When the concentration of hydrogen radicals is increased due to the presence of nickel catalyst, temperature has an even more dramatic effect on the products of CHP. From 350°C to 400°C, the yield of char drops from 54.6 C% to 44.4 C% and the yield of coke drops from 5.5 C% to 2.3 C%. The yield of known liquid decreases from 6.3 to 4.4 C% while the gas yield increases from 15.7 C% to 24.4 C%. At 350°C, the nickel catalyst prevents formation of carbon monoxide and carbon dioxide, with only a 2.1 C% yield of carbon dioxide and no carbon monoxide produced at all. At 400°C, the carbon dioxide yields disappear completely. Instead, methane increases from 6.1 C% to 22.6 C%. Conversely, other alkane gas yields decreased from 7.5 C% to 1.7 C%, suggesting that the high concentration of hydrogen radicals may lead to cleavage of single carbon-carbon bonds. Likewise, liquid alkanes decrease from 1.1 to 0.7 C%. Olefins were not produced at either temperature, which suggests that double carbon-carbon bonds are not kept intact at these conditions. Aromatics are not produced at all at 350°C but are produced in trace amounts at 400°C as they become more thermodynamically favorable at higher temperatures.

If the goal of CHP is to produce liquid hydrocarbons, nickel catalysts could help, as they increase the presence of hydrogen radicals that prevent deactivation by coking. However, the resulting methane needs to be recombined to produce the desired liquid hydrocarbons.

Effect of NiMo-ZSM-5 on CHP

It is possible that a methane dehydroaromatization (DHA) catalyst such as Mo-HZSM-5 could reconvert the methane to aromatic hydrocarbons. This reaction has been done without hydrogen; however, it was found that this catalyst is also deactivated by coking reactions [27,28]. These studies showed that DHA requires temperatures exceeding 600°C. We decided to try adding molybdenum to our Ni-HZSM-5 catalyst to verify the possibility of improving the yield of liquid hydrocarbons, despite our much lower reaction temperature. We hypothesized that the presence of hydrogen radicals could also promote this reaction. The results are shown in Figure 10.

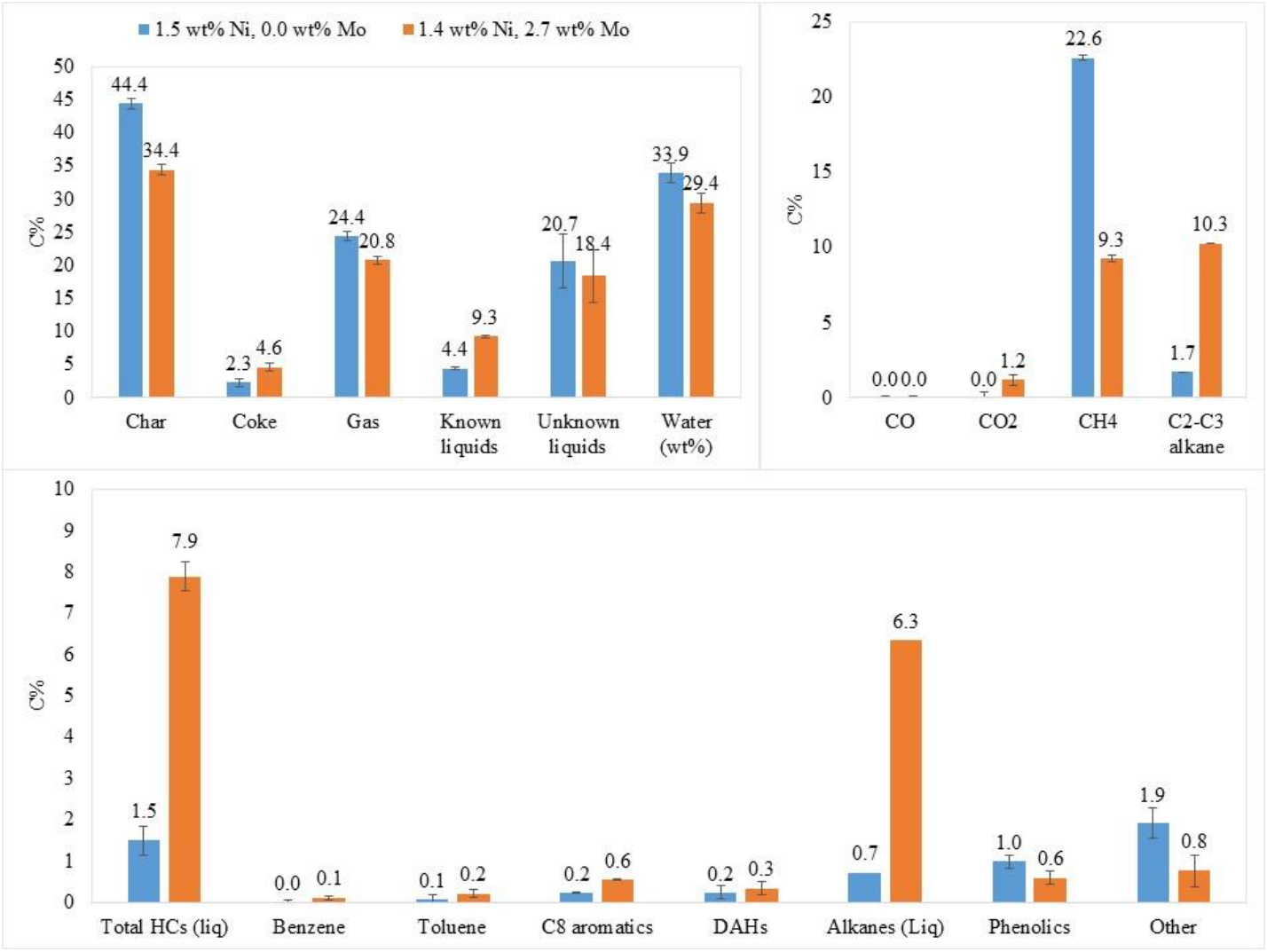

Figure 10: Effects of molybdenum sites on products of CHP. Top left: total yields. Top right: gaseous yields. Bottom: major liquid compounds. The carbon balances are 96.1 and 87.4 C%, respectively.

The yields of char and gas decreased with the addition of molybdenum to the Ni-HZSM-5, from 44.4 to 34.4 C% and from 24.4 to 20.8 C%. More of the carbon was consumed by the production of stable liquid hydrocarbons, preventing the secondary cracking and recombination reactions that affect the yields of CHP with just nickel on HZSM-5. Specifically, the yield of methane decreased from 22.6 to 9.3 C%. Instead, larger alkanes formed, either by a reduction in the extent of hydrogen radical cracking of alkanes, or by oligomerization of methane by the molybdenum sites. Ethane and propane yields increased from a combined 1.7 to 10.3 C%. Liquid

alkanes yields increased from 0.7 to 6.3 C%. The most abundant liquid alkanes are C5, yielding 2.4 C%. Most of these alkanes are cycloalkanes, with only a small amount of branched alkanes (2.4 C%).

Deoxygenation via HZSM-5 Analysis

Figure 11 shows the products of deoxygenation of pyrolysis vapors from A. Donax under various conditions with various forms of HZSM-5. The first two data points show that the nickel in the absence of hydrogen promotes decarboxylation and decarbonylation when compared to HZSM-5 in inert gas. The yield of hydrocarbons still increases slightly due to the ability of nickel to crack oxygenates to gases, including methane and light olefins. When hydrogen gas is introduced to HZSM-5 fast pyrolysis, the small concentration of hydrogen radicals is able to promote deoxygenation via decarbonylation and allows additional formation of hydrocarbons without significantly increasing the yield of water. Addition of nickel to the HZSM-5 in low amounts does not promote hydrodeoxygenation either but further reduces the extent of decarbonylation as well as decarboxylation. However, this leaves oxygen in the liquid products, reducing the yield of hydrocarbons. Adding more nickel eventually promotes hydrodeoxygenation at the expense of decarbonylation and decarboxylation reactions while efficiently removing oxygen from the liquids. When this happens, less carbon is consumed by CO_x gases and more carbon is available to be converted into hydrocarbons, though these are mostly gaseous. The addition of molybdenum did not have a large effect on how the oxygen is removed from the pyrolysis vapors, but it was able to promote more liquid hydrocarbons rather than gaseous hydrocarbons, likely by oligomerizing the gaseous alkanes.

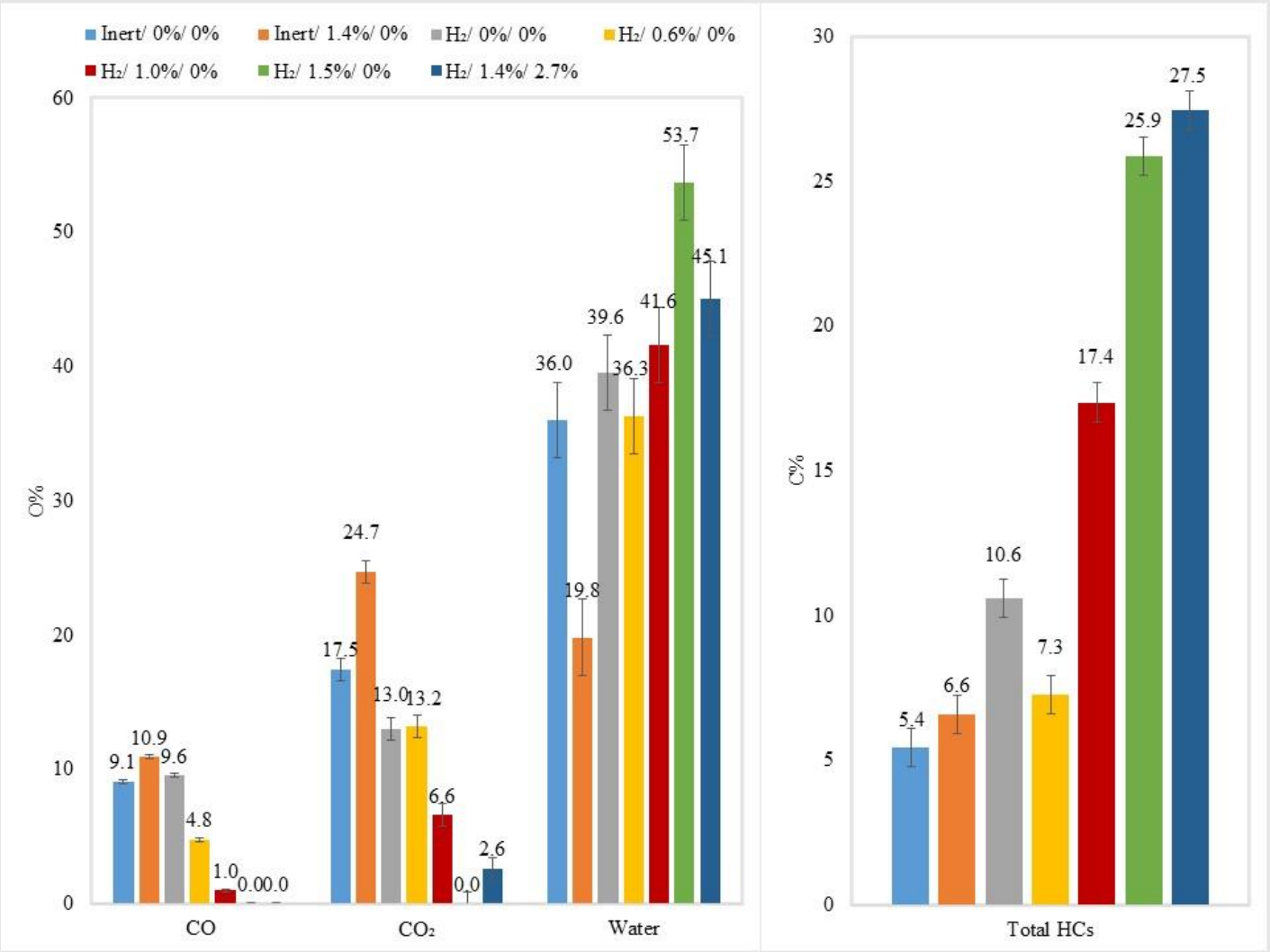

Figure 11: Products of biomass deoxygenation from CFP and CHP in O% with total hydrocarbons (liquid and gaseous) in C%.

This information allows us to expand upon Figure 1. Shows us the many new pathways that we provided evidence for in the present work. With increased heat, the absorbed organics produce more gaseous olefins such as ethylene. When hydrogen radicals are introduced, they promote desorption of the organics from the acid site, cracking of hydrocarbons to gases, methanation of carbon dioxide and carbon monoxide to water and methane, and cracking of all products to methane. Molybdenum sites promote reformation of the methane to higher carbon alkanes.

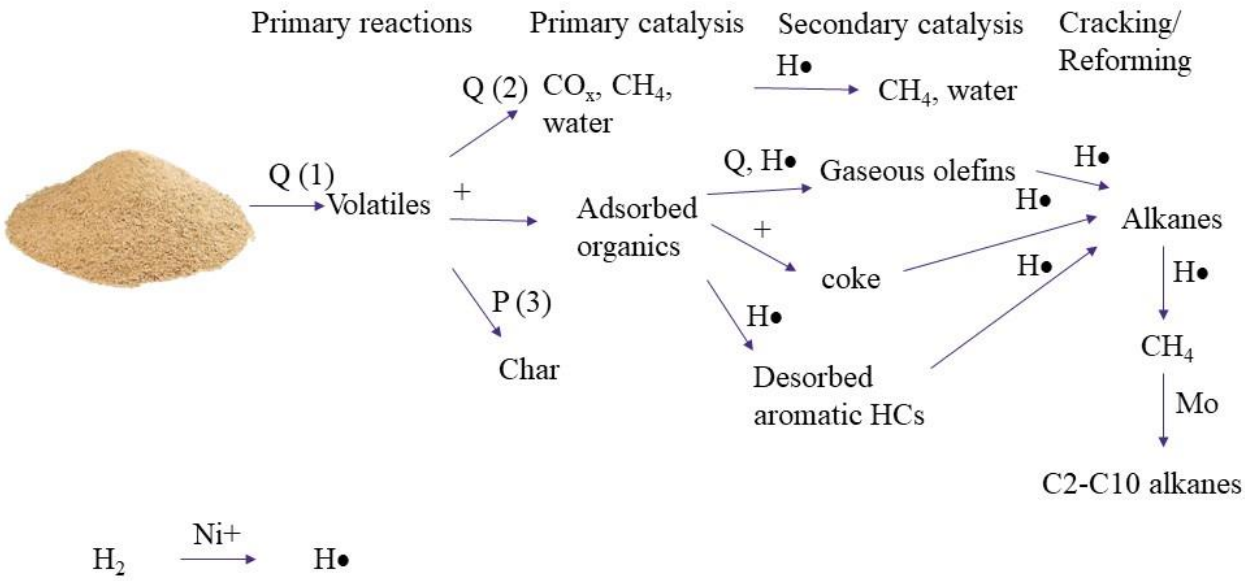

Analysis of Catalyst Post-run

Reaction gas	He	H_2	H_2	H_2
Catalyst	HZSM-5	HZSM-5	1.5 wt% Ni-ZSM-5	1.4 wt.% Ni, 2.7 wt% Mo-HZSM-5
Pre-run surface area (m^2/g)	279 ± 7.3	274.6	265	303.6
Biomass fed (g)	118.2	123.5	114	119.8
Coke mass yield (wt%)	6.77 wt.%	5.63 wt.%	2.07 wt.%	4.56%
Coke / g catalyst (g)	0.040	0.035	0.018	0.027
Post-run Surface area (m^2/g)	194.9	214.9	247.5	229.5
Surface area loss rate	50.9%	37.1%	11.6%	40.8%

Table 1: Results of BET analysis of catalyst before and after various experiments. Loss is defined in Equation 2

$$Surface\ area\ loss\ rate = \frac{\%\ surface\ area\ loss}{biomass\ to\ catalyst\ ratio} = \frac{1-(\frac{surface\ area\ after\ experiment}{surface\ area\ before\ experiment})}{\frac{total\ biomass\ fed\ in\ experiment}{total\ catalyst}}$$

Equation 2: Definition of surface area loss rate in units of % loss per gram biomass per gram catalyst

We performed BET analysis of the catalyst before and after some experiments. The results are shown in Table 1. Surface area and pore volume each decreases with increasing amounts of coke on the catalyst. Therefore, conditions that produce less coke, like CHP with Ni-HZSM-5, would better preserve the original properties of the catalyst.

Conclusion

We performed catalyst fast pyrolysis of *A. Donax* with HZSM-5 at varying temperatures, weight hour space velocities, and pressures with and without hydrogen gas, nickel active sites, and molybdenum active sites. The highest yield of liquid hydrocarbons were produced with HZSM-5 catalyst at 550°C and 1 bar in pure nitrogen gas. However, the highest yield of total hydrocarbons, including gas, was produced by the NiMo-HZSM-5 at 400°C and 35 bar in pure hydrogen gas, demonstrating that this catalyst has the most potential to produce liquid transportation fuels at the proper conditions.

Changing the weight hourly space velocity had little effect on the products of CFP until we exceeded 1.9 hr^{-1}, at which point, the lack of available active sites prevented deoxygenation. Increasing the temperature decreased the yields of liquid hydrocarbons by cracking to gas. Reducing the temperature promoted recombination reactions to char. Introduction of hydrogen gas at 400°C increased the yield of liquid hydrocarbons by reducing the rate of coking. Decreasing the temperature reduced this effect and reduced the yields of liquid hydrocarbons. Adding nickel to the catalyst weakened the diatomic hydrogen bonds producing more hydrogen radicals, which reduced coking further, but cracked the liquid hydrocarbons into alkane gases,

especially methane. Decreasing the temperature with Ni-HZSM-5 reduced this effect, but still did not improve liquid hydrocarbon yields. Finally, the addition of molybdenum to the Ni-HZSM-5 prevented the cracking of liquid hydrocarbons, allowing liquid cycloalkanes to form. Furthermore, this catalyst produced a mixture of aromatic hydrocarbons and cycloalkanes, whereas without hydrogen, all liquid hydrocarbons were aromatic, which is not suitable as a standalone fuel.

Future work

A study comparing the yields of CHP with NiMo-HZSM-5 at varying temperatures and pressures could show that this catalyst has more potential for the production of liquid transportation fuels. This pathway could greatly improve the quality of transportation fuels from catalytic fast pyrolysis. In the future, we plan to use the fluidized bed reactor with Ni-HZSM-5 at higher temperatures (450-550°C) to produce methane from lignocellulosic biomass. A secondary fixed bed reactor with NiMo-HZSM-5 would then recombine the methane to liquid transportation fuels. We hope to study the effects of temperature, nickel loading, and molybdenum loading on this process and aim to maximize the yields of liquid hydrocarbon from catalytic fast hydropyrolysis. This would have a major impact on the availability of sustainable transportation fuels and help to alleviate the issues associated with the continued use of petroleum fuels.

References

[1] C. Williams, T. Biswas, A. Downie, Yield , salt tolerance and energy from Arundo donax : a potential biochar and biofuel crop, in: 1st Asia Pacific Biochar Conf., Queensland, AU, 2009.

[2] J. Giessow, Jason; Casanova, Jason; Leclerc, Rene; MacArthur, Robert;Fleming, Genie;Giessow, Arundo Distribution and Impact Report, (2011).

[3] A. V Bridgwater, Fast Pyrolysis of Biomass for Energy and Fuels, (n.d.).

[4] T.R. Carlson, Y.-T. Cheng, J. Jae, G.W. Huber, Production of green aromatics and olefins by catalytic fast pyrolysis of wood sawdust, Energy Environ. Sci. 4 (2011) 145–161. doi:10.1039/C0EE00341G.

[5] S. Meesuk, J.P. Cao, K. Sato, Y. Ogawa, T. Takarada, Fast pyrolysis of rice husk in a fluidized bed: Effects of the gas atmosphere and catalyst on Bio-oil with a relatively low content of oxygen, Energy and Fuels. 25 (2011) 4113–4121. doi:10.1021/ef200867q.

[6] S. Thangalazhy-Gopakumar, S. Adhikari, R.B. Gupta, M. Tu, S. Taylor, Production of hydrocarbon fuels from biomass using catalytic pyrolysis under helium and hydrogen environments, Bioresour. Technol. 102 (2011) 6742–6749. doi:10.1016/j.biortech.2011.03.104.

[7] O. Jan, R. Marchand, L.C.A. Anjos, G.V.S. Seufitelli, E. Nikolla, F.L.P. Resende, Hydropyrolysis of lignin using Pd/HZSM-5, Energy and Fuels. 29 (2015) 1793–1800. doi:10.1021/ef502779s.

[8] F. Melligan, M.H.B. Hayes, W. Kwapinski, J.J. Leahy, Hydro-pyrolysis of biomass and online catalytic vapor upgrading with Ni-ZSM-5 and Ni-MCM-41, Energy and Fuels. 26 (2012) 6080–6090. doi:10.1021/ef301244h.

[9] F. Melligan, M.H.B. Hayes, W. Kwapinski, J.J. Leahy, A study of hydrogen pressure during hydropyrolysis of Miscanthus x giganteus and online catalytic vapour upgrading

with Ni on ZSM-5, J. Anal. Appl. Pyrolysis. 103 (2013) 369–377. doi:10.1016/j.jaap.2013.01.005.

[10] D. Radlein, A. Quignard, Une bréve revue historique de la pyrolyse rapide de la biomasse, Oil Gas Sci. Technol. 68 (2013) 765–783. doi:10.2516/ogst/2013162.

[11] D.S. Scott, J. Piskorz, The Continuous Flash Pyrolysis of Biomass, Can. J. Chem. Eng. 62 (1984) 404–412.

[12] M. Olazar, R. Aguado, J. Bilbao, A. Barona, Pyrolysis of sawdust in a conical spouted-bed reactor with a HZSM-5 catalyst, AIChE J. 46 (2000) 1025–1033. doi:10.1002/aic.690460514.

[13] F.L.P. Resende, Recent advances on fast hydropyrolysis of biomass, Catal. Today. 269 (2016) 148–155. doi:10.1016/j.cattod.2016.01.004.

[14] D.P. Gamliel, L. Wilcox, J.A. Valla, The effects of catalyst properties on the conversion of biomass via catalytic fast hydropyrolysis, Energy and Fuels. 31 (2017) 679–687. doi:10.1021/acs.energyfuels.6b02781.

[15] D.P. Gamliel, G.M. Bollas, J.A. Valla, Bifunctional Ni-ZSM-5 Catalysts for the Pyrolysis and Hydropyrolysis of Biomass, Energy Technol. 5 (2017) 172–182. doi:10.1002/ente.201600136.

[16] D.P. Gamliel, G.M. Bollas, J.A. Valla, Two-stage catalytic fast hydropyrolysis of biomass for the production of drop-in biofuel, Fuel. 216 (2018) 160–170. doi:10.1016/j.fuel.2017.12.017.

[17] S. Thangalazhy-Gopakumar, S. Adhikari, R.B. Gupta, Catalytic pyrolysis of biomass over

H +ZSM-5 under hydrogen pressure, Energy and Fuels. 26 (2012) 5300–5306. doi:10.1021/ef3008213.

[18] D.C. Dayton, J. Hlebak, J.R. Carpenter, K. Wang, O.D. Mante, J.E. Peters, Biomass Hydropyrolysis in a Fluidized Bed Reactor, Energy and Fuels. 30 (2016) 4879–4887. doi:10.1021/acs.energyfuels.6b00373.

[19] T.L. Marker, L.G. Felix, M.B. Linck, M.J. Roberts, Integrated hydropyrolysis and hydroconversion (IH2) for the direct production of gasoline and diesel fuels or blending components from biomass, part 1: Proof of principle testing, Environ. Prog. Sustain. Energy. 31 (2012) 191–199. doi:10.1002/ep.10629.

[20] E.C.D. Tan, T.L. Marker, M.J. Roberts, Direct Production of Gasoline and Diesel Fuels from Biomass via Integrated Hydropyrolysis and Hydroconversion Process—A Techno-economic Analysis, Environ. Prog. Sustain. Energy. 33 (2014) 609–617. doi:10.1002/ep.11791.

[21] T.L. Marker, L.G. Felix, M.B. Linck, M.J. Roberts, P. Ortiz-Toral, J. Wangerow, Integrated Hydropyrolysis and Hydroconversion (IH^2) for the Direct Production of Gasoline and Diesel Fuels or Blending Components from Biomass, Part 2: Continuous Testing, Environ. Prog. Sustain. Energy. 33 (2014) 762–768. doi:10.1002/ep.

[22] A. Sluiter, B. Hames, R. Ruiz, C. Scarlata, J. Sluiter, D. Templeton, Determination of ash in biomass: Laboratory Analytical Procedure (LAP), 2008. doi:NREL/TP-510-42619.

[23] EPA, Determination of metals and trace elements in water and wastes by inductively coupled plasma-atomic emission spectrometry, Method 200.7. Revision 4 (1994) Revision 4.4.

[24] G. Luo, D.S. Chandler, L.C.A. Anjos, R.J. Eng, P. Jia, F.L.P. Resende, Pyrolysis of whole wood chips and rods in a novel ablative reactor, Fuel. 194 (2017). doi:10.1016/j.fuel.2017.01.010.

[25] D.S. Chandler, F.L.P. Resende, Effects of warm water washing on the fast pyrolysis of Arundo Donax, Biomass and Bioenergy. 113 (2018) 65–74. doi:10.1016/j.biombioe.2018.03.008.

[26] D. Dandy, Chemical Equilibrium Calculation, Color. State Univ. Bioanal. Microfluid. Progr. (2018). http://navier.engr.colostate.edu/code/code-4/index.html.

[27] Z.R. Ismagilov, E. V. Matus, L.T. Tsikoza, Direct conversion of methane on Mo/ZSM-5 catalysts to produce benzene and hydrogen: achievements and perspectives, Energy Environ. Sci. 1 (2008) 526. doi:10.1039/b810981h.

[28] L.Y. Chen, L. Lin, Z. Xu, X. Li, T. Zhang, Dehydro-oligomerization of methane to ethylene and aromatics over molybdenum/HZSM-5 catalyst, J. Catal. 157 (1995) 190–200. doi:10.1006/jcat.1995.1279.